DEVELOPMENT OF A GAMMAGRAPHY SYSTEM FOR UNDERWATER PIPELINES INSPECTION

Oliveira, Davi Ferreira, davi@lin.ufrj.br
Lopes, Ricardo Tadeu, ricardo@lin.ufrj.br
PEN/COPPE/UFRJ - Av. Horácio Macedo, 2030, Bloco I, Sala 133 – Rio de Janeiro, RJ – Brazil

Marinho, Carla Alves, carlamarinho@petrobras.com.br
CENPES/PETROBRAS – Av. Horácio Macedo, 950 – Rio de Janeiro, RJ – Brazil

Camerini, Claudio Soligo, claudiocamerini@petrobras.com.br
CENPES/PETROBRAS – Av. Horácio Macedo, 950 – Rio de Janeiro, RJ – Brazil

Abstract. *Owing to the growing utilization of underwater pipelines, a great need to study possible means of evaluating the structural integrity of these pipelines has arisen. Currently, underwater pipelines are inspected in a similar manner to land pipelines, using the so-called instrumented pigs, this being the only tool used for decision making on the conditions of a pipepline's operational continuity. However, the results generated by a pig are only capable of indicating the existence of the defect, but not of quantifying it. Thus, the main objective of this work is to develop an inspection system using the computed radiography technique (CR) in order to carry out further analysis on the passage of instrumented pigs with good image quality, producing reliable results about the conditions of the ducts inspected. The motivation for the development and application of these CR tests originated in the record of atypical signals in the lower generatrix of the circumferential girth welds of three pipelines, a result which was obtained through the inspection with MFL pigs. The occurrence became critical due to the great number of welded joints presenting such indications. Due to the need of characterizing the problem, an inspection of some spots from each pipeline was performed through underwater gammagraphy, using a tool handled by divers and a computed radiography system. In order to calibrate the system for greater accuracy of results, specimens of equal size to the three pipelines containing girth welds with corrosion alveoli in various depths were inspected in the laboratory. The inspection setup was similar to the inspection of field tests. The results obtained revealed that the indications refer to damages by localized internal corrosion, showing mass loss between 10% and 28% of thickness. This observation was the same for the three pipelines.*

Keywords*: Underwater Pipeline Inspection, Computed Radiography, Corrosion Monitoring*

1. INTRODUCTION

Owing to the growing utilization of underwater pipelines, a great need to study possible means of evaluating the structural integrity of these pipelines has arisen. Currently, underwater pipelines are inspected in a similar manner to land pipelines, using the so-called instrumented pigs, this being the only tool used for decision making on the conditions of a pipeline's operational continuity (Marinho *et al*., 2006). However, the results generated by a pig are only capable of indicating the existence of the defect, but not of quantifying it.

Since more than 100 years industrial radiology is based on X-ray film. Special film systems have been developed for NDT applications, which have better image quality than medical film systems but lower speed. High spatial resolution is obtained by combination of these films with lead screens instead of fluorescence screens (Ewert, 2002).

Direct digitizing systems accelerate the process of intelligent digital radiology. Since almost 10 years imaging plate systems are available which can be used as filmless radiography technique, also known as computed radiography (CR). Imaging plates can be exposed and scanned by a laser scanner to obtain a digital radiograph. They can be erased by an optical process and be reused up to 1000 times (Ewert, 2002).

The main objective of this work is to develop an inspection system using the computed radiography technique in order to carry out further analysis on the passage of instrumented pigs with good image quality, producing reliable results about the conditions of the ducts inspected.

2. MATERIALS AND METHODS

2.1. Underwater Gammagraphy System

This system is a mechanic device, comprising a basket of steel, where the radioactive source is introduced and an envelope of polyurethane, which is inserted the detector (image plate). The system is adjustable, allowing the inspections to be executed in a wide range of pipelines diameters. The geometry of the device was developed so that the radiographs could be performed with the double wall single image (DWSI) technique.

The source (Ir-192) is placed in a conventional irradiator and the set is "marinized" through a stainless steel vase, and can be operated up to 1,800 m deep. The source is exposed through a surface controller via coaxial cable, currently 200 m long. Figure 1 shows the irradiator, the "marinized" stainless steel vase and the exposure controller.

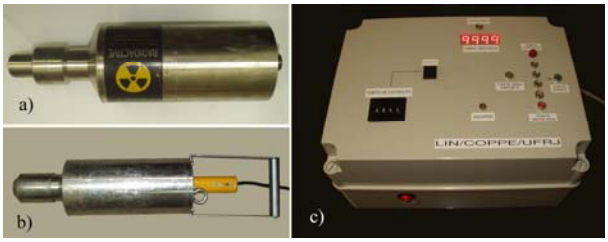

Figure 1. a) irradiator, b) irradiator in the marinized vase e c) exposure controller.

The industrial computed radiography equipment used was CR50P, manufactured by GEIT. For the acquisition and the images processing it was used the Rhythm Acquire and Rhythm Review softwares, respectively. This system has a range of gray levels that ranges from 0 to 49,140, scanning the image plate with laser spot size of 50 μm and generate images with pixel sizes that ranges from 50 to 200 μm. After the scanning, the image plate is erased by the system and is ready for a new radiographic exposure. Figure 2 shows the industrial computed radiography equipment CR50P.

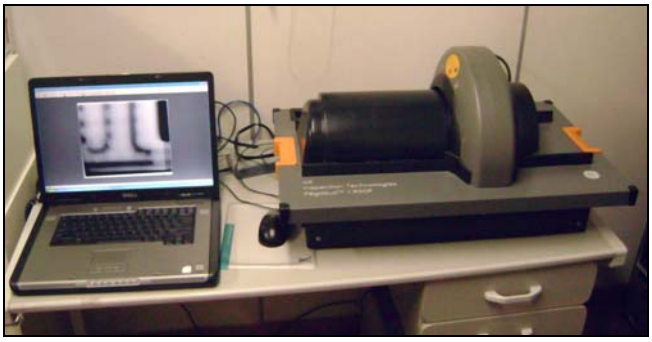

Figure 2. Industrial computed radiography equipment GE CR50P.

The detector employed was manufactured by GE-IT, model IPC2 Black. In these inspections, lead intensifying screens were also used to reduce the scattered radiation. The set was protected from contact with water through envelopes of waterproof plastic, sealed with a sealing machine.

Before positioning the irradiator in the mechanical device it is inserted a lead collimator suitable for geometry of the irradiator, which ensures that the beam of gamma rays is confined in the region of interest for inspection. Figure 3 (a) outlines the radiographic exposure, while Figure 3 (b) shows that the steel basket of the mechanical device displays a window, which coincides with the window of the lead collimator.

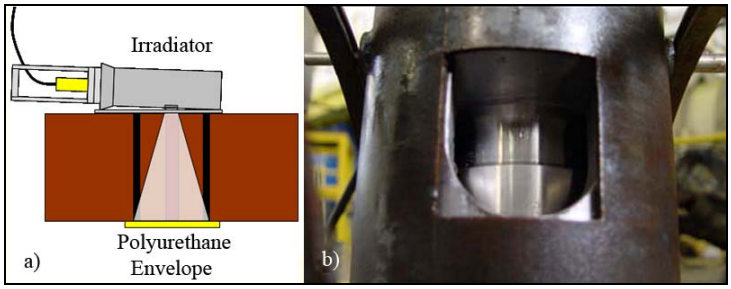

Figure 3. a) Illustration of radiographic exposure and b) window for irradiation of the basket with the lead collimator.

2.2. Assembly of the Radiographic Setup

First the diver places the mechanic device on the spot of interest, observing the positioning of the basket on the weld bead and the alignment of the radioactive source and the polyurethane envelope. The sealed imaging plate is inserted in the polyurethane and the mechanic device is set on the pipeline's diameter. Then there is the assembly of the lead collimator and, finally, the placing of the irradiator in the basket. At the end of the assembly, the diver moves to a

security distance (over 1m) and the radiographic exposition begins through the surface controller. The described procedure was the same in all inspected spots, and Figure 4 shows stills of this assembly.

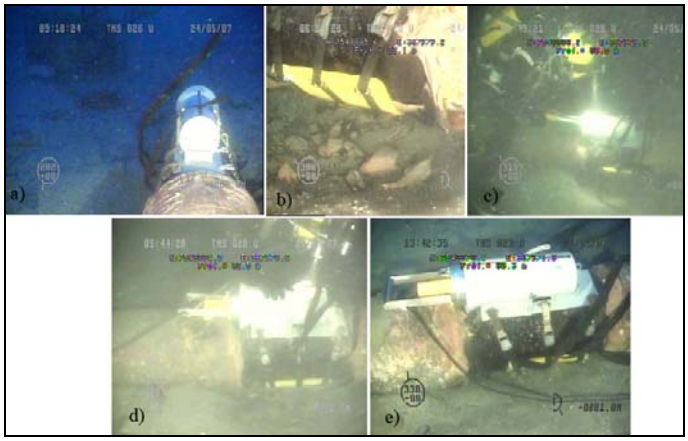

Figure 4. (a) Positioning of the iron basket; (b) Positioning of the plate; (c) Diver placing the irradiator in the basket; (d) Diver checking the placement of the irradiator; (e) Exposition.

2.3. Inspection Spots

The inspections were executed in three pipelines located in the Campos Basin, corresponding lines PVM1-PVM2, PVM2-PVM3 and PVM3-PPG1. The pipelines are made of steel and have thicknesses of approximately 11 mm. The depth in the implementation of the work was about 80 m. Images were obtained from seven different spots and the exposure times were adjusted for each spot, due to the passage or not of oil inside the pipeline at the moment of radiography. Table 1 shows the diameters of each line and the exposure time used in each spot. The activity of Ir-192 source was 2.15 TBq and the focal spot size was 2.95 mm.

Table 1. Parameters of exposure

Line	Spot	Diameter (inch)	Exposure Time (s)
PVM1-PVM2	1	10	3600
PVM1-PVM2	2	10	1800
PVM2-PVM3	3	12	3000
PVM2-PVM3	4	12	4500
PVM3-PPG1	5	16	9000
PVM3-PPG1	6	16	7200
PVM3-PPG1	7	16	9000

3. RESULTS

3.1. Measurement of Residual Thickness

Despite the observation of the existence of a corrosive process located in the girth welds of the pipelines, the residual thicknesses were not quantified immediately, and can only determine the nature of the defects identified by MFL pigs. For a quantitative evaluation of the results it was necessary a second stage at the laboratory, which were made simulations of the field conditions in samples showing similar characteristics to the pipelines inspected. Each of these samples was transversely cut and their halves were welded, afterwards notch-like defects were made in circumferential welds representing loss of thickness of 20, 30, 40, 50, 60, 70, 80 and 100%.

The expositions were made in immersion tanks, and the periods of exposition were set in such a way that the images obtained presented, in some uniform region in the welded joint, signal intensities (gray level) of the same order as those joints observed in the field. When this level was achieved, the assessments were then made through two methods: assessment of the effective absorption coefficient and linear interpolation.

Firstly, using the samples tested in the laboratory, the effective absorption coefficient in each spot was determined. Then, the average of the coefficients for each diameter was obtained, and with these values, the depth of the defects of the field samples was determined. Table 2 shows the mean values found for the three diameters mentioned.

Table 2. Effective absorption coefficient for the three diameters.

Pipeline Diameter (inch)	Effective Absorption Coefficient (mm^{-1})	Standard Deviation
10	0.035	0.00013
12	0.026	0.00016
16	0.020	0.00024

The second evaluation method used was the linear interpolation. From the images with the calibration samples it was obtained the gray values in the region of weld without defect and at each defect corresponding to a percentage of loss thickness. With the equations obtained, it was possible to determine the mass loss due to corrosion in the field samples.

To analyze the images of the field samples, the defects were divided into regions according to their homogeneity. For this evaluation, profiles were plotted, showing the gray values along a marked line on the defect. With the profile line, it was possible to visualize the areas where the gray values present lower difference and thus sharing the defects in regions of interest.

3.2 – Line PVM1-PVM2

Figures 5 and 6 show the images with the marking of the line profiles on the defects and their respective measurement length, the graphics of the line profiles for the marking of regions of minor discrepancies in gray values of the defect and the identification of regions of loss thickness for spots 1 and 2, respectively.

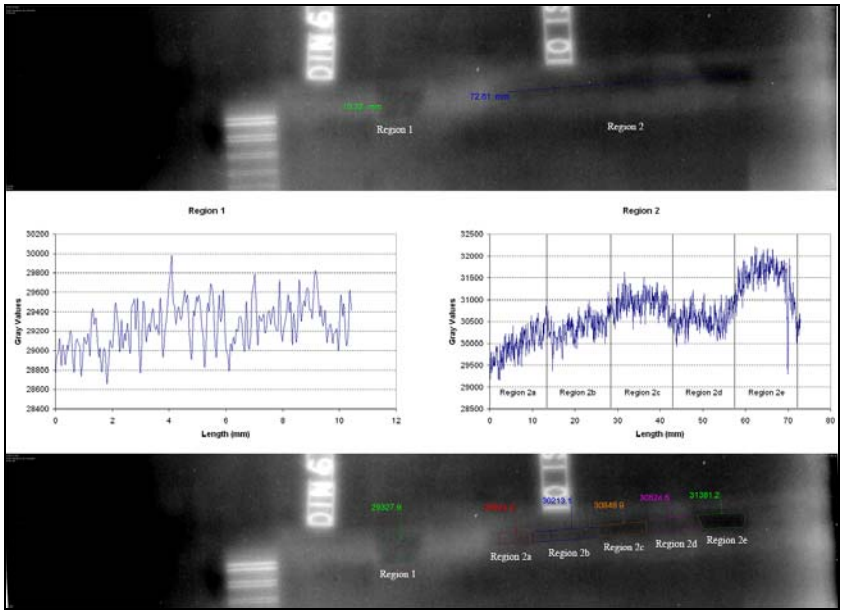

Figure 5. Image and analysis of the spot 1.

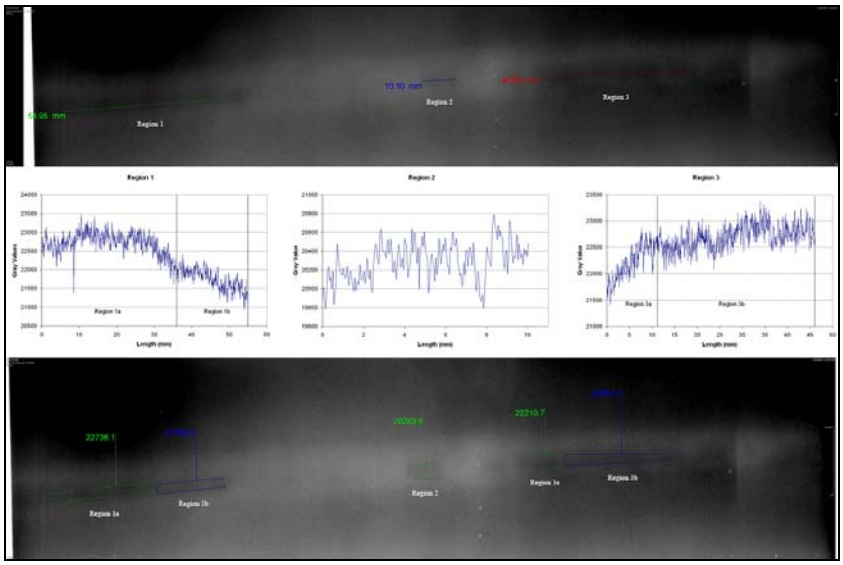

Figure 6. Image and analysis of the spot 2.

Tables 3 and 4 show the results of wall loss analysis using the two methods for the inspection spots 1 and 2, respectively.

Table 3. Wall loss value determined by the methods of interpolation and effective absorption coefficient for the spot 1.

Wall Loss (%)		
	Interpolation	Effective Absorption Coefficient
Region 1		
a	8.50	8.31
Region 2		
a	10.25	10.72
b	13.73	14.66
c	17.48	18.59
d	15.56	16.48
e	20.62	22.54

Table 4. Wall loss value determined by the methods of interpolation and effective absorption coefficient for the spot 2.

Wall Loss (%)		
	Interpolation	Effective Absorption Coefficient
Region 1		
a	24.63	24.64
b	15.61	16.31
Region 2		
a	1.82	1.83
Region 3		
a	19.74	19.50
b	23.65	23.95

3.3. Line PVM2-PVM3

Figures 7 and 8 show the images with the markings of line profiles on the defects and their respective measurement length, the graphics of the line profiles for marking regions of minor discrepancies in the gray values of the defect and the identification of regions of loss thickness for spots 3 and 4, respectively.

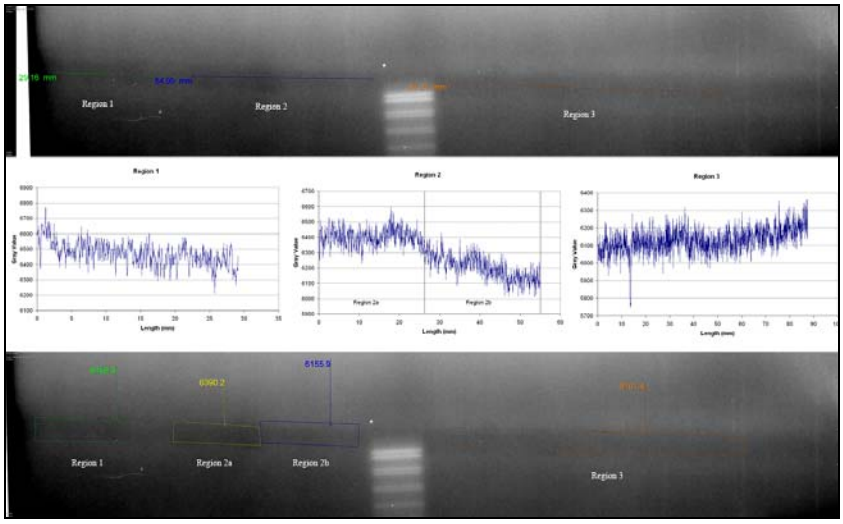

Figure 7. Image and analysis of the spot 3.

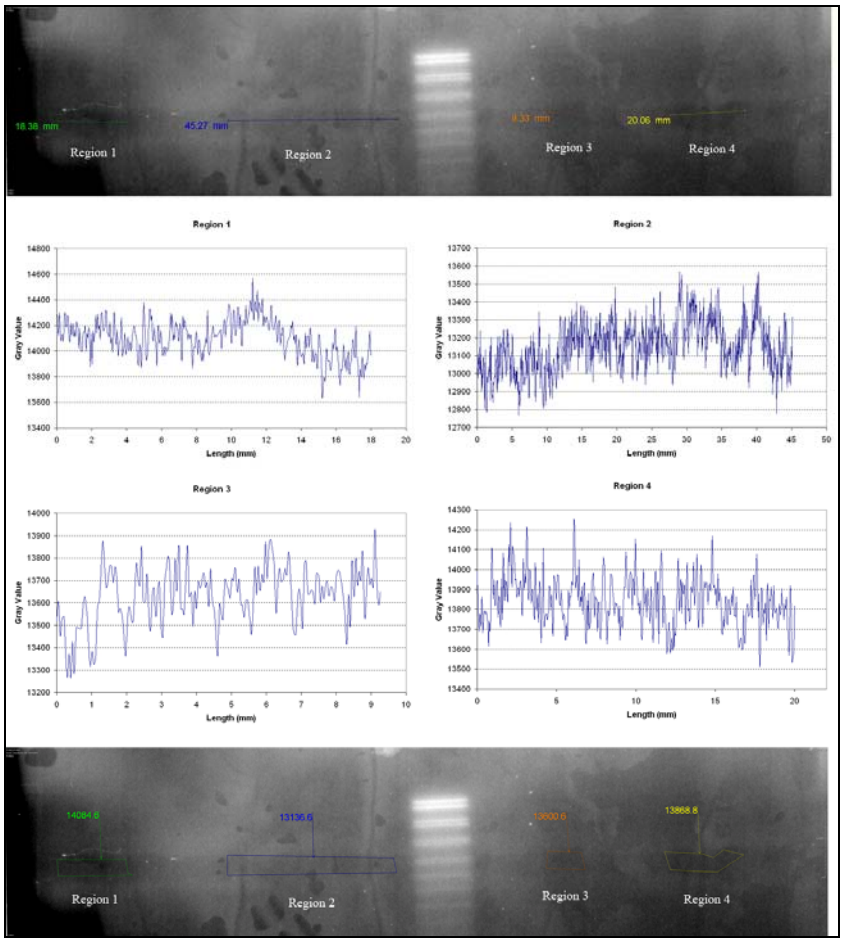

Figure 8. Image and analysis of the spot 4.

Tables 5 and 6 show the results of wall loss analysis using the two methods for the inspection spots 3 and 4, respectively.

Table 5. Wall loss value determined by the methods of interpolation and effective absorption coefficient for the spot 3.

Wall Loss (%)		
	Interpolation	Effective Absorption Coefficient
Region 1		
a	26.80	28.20
Region 2		
a	24.57	26.82
b	16.67	16.88
Region 3		
a	14.84	12.87

Table 6. Wall loss value determined by the methods of interpolation and effective absorption coefficient for the spot 4.

Wall Loss (%)	
Interpolation	Effective Absorption Coefficient
Region 1	
26.12	28.34
Region 2	
11.52	10.02
Region 3	
18.67	18.16
Region 4	
22.80	24.18

3.4. Line PVM3-PPG1

Figures 9, 10 and 11 show the images with the markings of line profiles on the defects and their respective measurement length, the graphics of the line profiles for marking regions of minor discrepancies in the gray values of the defect and the identification of regions of loss thickness for spots 5, 6 and 7, respectively.

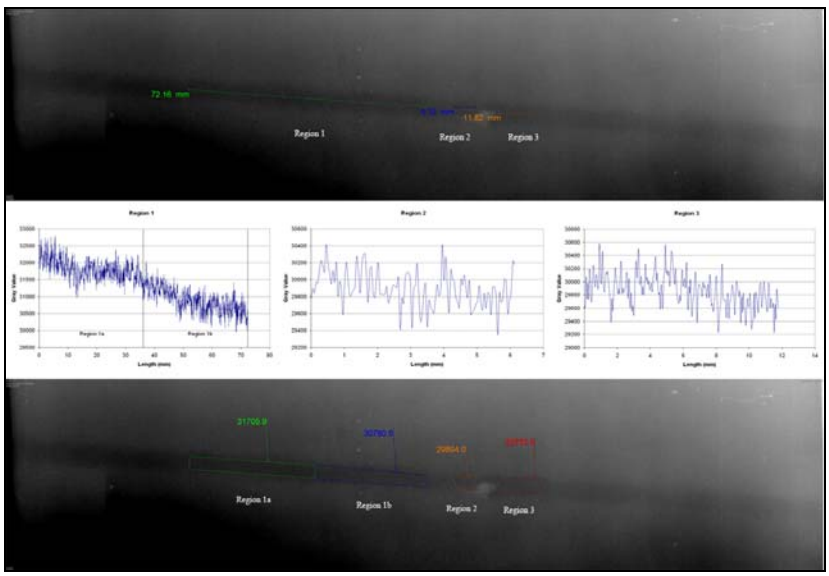

Figure 9. Image and analysis of the spot 5.

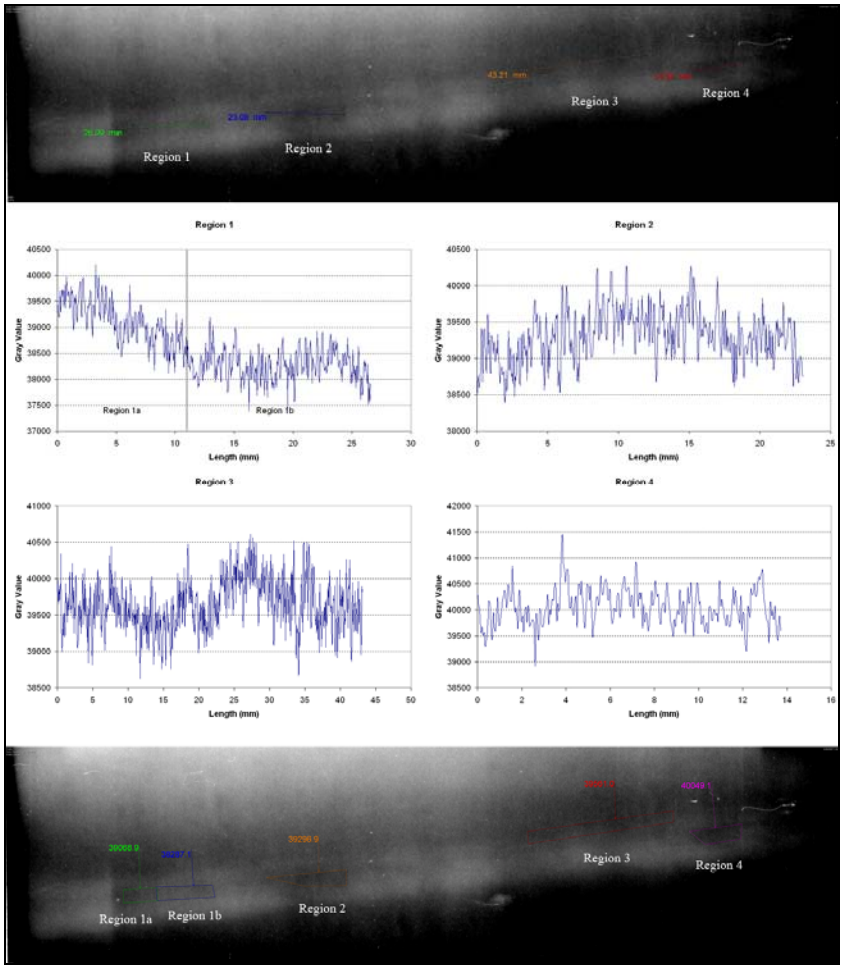

Figure 10. Image and analysis of the spot 6.

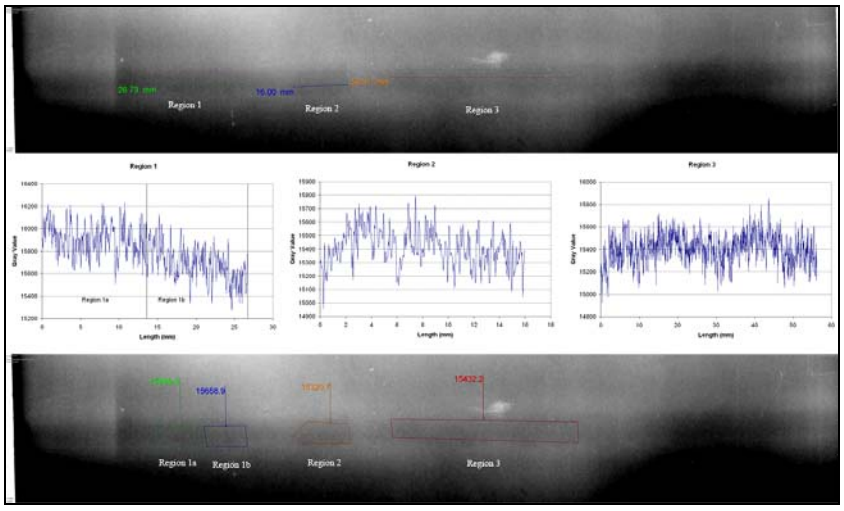

Figure 11. Image and analysis of the spot 7.

Tables 7, 8 and 9 show the results of wall loss analysis using the two methods for the inspection spots 5, 6 and 7, respectively.

Table 7. Wall loss value determined by the methods of interpolation and effective absorption coefficient for the spot 5.

Wall Loss (%)		
	Interpolation	Effective Absorption Coefficient
Region 1		
a	9.68	10.85
b	8.15	10.24
Region 2		
a	9.59	11.34
Region 3		
a	8.37	10.29

Table 8. Wall loss value determined by the methods of interpolation and effective absorption coefficient for the spot 6.

Wall Loss (%)		
	Interpolation	Effective Absorption Coefficient
Region 1		
a	16.13	16.03
b	11.21	11.41
Region 2		
a	17.57	16.97
Region 3		
a	19.23	18.79
Region 4		
a	22.31	23.65

Table 9. Wall loss value determined by the methods of interpolation and effective absorption coefficient for the spot 7.

Wall Loss (%)		
	Interpolation	Effective Absorption Coefficient
Region 1		
a	21.59	24.90
b	17.42	18.10
Region 2		
a	11.57	13.67
Region 3		
a	13.50	16.91

4. CONCLUSIONS

The results obtained showed that in the lower generatrix of the girth welds of the pipelines present unquestionable mass loss, without traces of intense corrosive process in the metal of adjacent basis. This observation was the same for the three pipelines.

The corrosion displayed more punctual occurrence in the welded joints of spots 1, 2 and 6 and more uniform in spots 3, 4, 5 and 7, but, with regions of greater relative loss of thickness in all cases.

The loss of thickness measured ranged predominantly from 10 to 28% on the pipeline walls. The causes for this loss demand further study and involvement of corrosion experts.

A reassessment of the signal intensities displayed by the MFL pigs must be made in the inspected spots, so as to determine how many indications are in similar or worse situation, in order to realize the extension of the problem in the pipelines and the importance of the selected spots.

The inspection service performed is unique in this country, and there is no account of similar procedure overseas.

5. ACKNOWLEDGEMENTS

To diving inspectors Ricardo Vargas and Jorge, as well as *Toisa Sentinel* crew. To the Fugro Marsat team, and specially to divers involved in this work.

This work was partially supported by Conselho Nacional de Desenvolvimento Científico e Tecnológico (CNPq), Fundação Carlos Chagas Filho de Amparo Pesquisa do Estado do Rio de Janeiro (FAPERJ) and Coordenação de Aperfeiçoamento de Pessoal de Nível Superior (CAPES).

6. REFERENCES

Ewert, U., 2002, "Upheaval in Industrial Radiology", Proceedings of the 8th European Conference on Nondestructive Testing, Barcelona, Spain.

Marinho, C. A. et al, 2006, "Novas Aplicações da Técnica de Radiografia Computadorizada em Ambiente Offshore", Proceedings of the 24th Congresso Nacional de Ensaios Não Destrutivos e Inspeção, São Paulo, Brazil.

Marinho, C.A. et al, 2008, "Gamma Ray System Operated by Divers for Underwater Inspection", Proceedings of the 17th World Conference on Nondestructive Testing, Shanghai, China.

7. RESPONSIBILITY NOTICE

The authors are the only responsible for the printed material included in this paper.